CHAPTER V

ADVANCED ROBUST DISTURBANCE-REJECTION CONTROL DESIGN FOR QUADROTOR UAV SYSTEMS IN TRACKING AGGRESSIVE TRAJECTORIES

Yakoub NETTARI

(Assist. Prof. Dr.) Electrical Engineering Department,
Istanbul Sabahattin Zaim University, Halkalı Cad. No: 281 Halkalı
Küçükçekmece, Istanbul, 34303, Turkey
E-mail: yakup.cezayirli@izu.edu.tr
ORCID: 0000-0002-6426-0632

1. Introduction

Unmanned aerial vehicles (UAVs), commonly known as drones, have seen significant progress as a result of advancements in embedded systems, actuators, sensors, and control algorithms. Their versatility has led to widespread use in civilian and military applications, such as environmental monitoring, agriculture, delivery services, and disaster management (Hassanalian & Abdelkefi, 2017; H. Liu et al., 2017; Mu et al., 2017; Shakhatreh et al., 2019). A notable UAV type is the quadrotor, which uses four rotors and offers advantages over traditional helicopters, including more straightforward maintenance, easier attitude control, and a compact design (Hoffmann et al., 2011). However, quadrotors face challenges like high nonlinearity, sensitivity to wind gusts, and parameter uncertainties, making flight controller design complex (Ai & Yu, 2019; Hua et al., 2018; Zou & Zhu, 2017; Zuo & Ru, 2014).

Over the past decade, numerous control strategies for quadrotors have been proposed to ensure accurate trajectory tracking and target achievement. These approaches include sliding mode control (Yang et al., 2018), nonlinear PID controllers (Moreno-Valenzuela et al., 2018), model predictive control (Alexis et al., 2014), flatness-based control (Aguilar-Ibáñez et al., 2012; Chamseddine et al., n.d.), adaptive trajectory tracking (Antonelli et al., 2018),

active disturbance rejection (Bouzid et al., 2017), and robust generalized dynamic inversion (Ansari et al., 2019). Other advanced methods, such as adaptive terminal sliding mode (H. Wang et al., 2016), immersion and invariance (Zhao et al., 2015), and hybrid finite-time control (Labbadi & Cherkaoui, 2019; N. Wang et al., 2019), have also been explored to address the system's nonlinearity and disturbances. Super-twisting algorithms (STA) have gained prominence as effective controllers for nonlinear systems, offering chattering reduction and robustness, with applications in sliding mode control, adaptive systems, and fractional-order approaches (Labbadi et al., 2020; Nettari et al., 2023).

Early quadrotor development showed that linear controllers could ensure stable flight (Hoffmann et al., n.d.), including PID, linear quadratic (Bouabdallah, Murrieri, et al., 2004; Bouabdallah, Noth, et al., 2004; Bouabdallah & Siegwart, 2005), and H∞ controllers (Hamza et al., 2022). However, due to the system's nonlinear and underactuated nature, achieving better performance requires robust and intelligent control techniques (Kim et al., 2021).

Numerous studies have explored intelligent control for quadrotors. Switching model predictive control (SMPC) was applied to quadrotors (Alexis et al., 2014), although it requires a precise prediction model. The concept of fuzzy logic, introduced by Zadeh (Zadeh, 1965), has been widely developed, with Coza and Macnab (Coza & Macnab, n.d.) demonstrating its stability through adaptive fuzzy control. Neural network applications in quadrotor control were explored by Dierks and Jagannathan (Dierks & Jagannathan, 2010), While fuzzy logic lacks practical training data (Katic et al., 2005), its solutions are human-understandable, unlike neural networks (Kim et al., 2021). Given the limitations of intelligent control methods, this study focuses on robust strategies, including nonlinear PD (Dong et al., 2016), feedback linearization (Lee et al., 2009), backstepping control, and sliding mode control (Bouabdallah & Siegwart, 2005a, 2007; Shao et al., 2018). Authers in (Altuğ et al., 2005) compared feedback linearization and backstepping, finding better performance with the backstepping controller.

Robust controllers are essential for high-precision positioning due to uncertainties and external disturbances. A robust adaptive control technique is provided in (Antonelli et al., 2018) to handle these factors. A continuous sliding mode controller for trajectory tracking in a swarm of quadrotors is introduced in (González-Sierra et al., 2020). For nonlinear underactuated quadrotors, direct control is unsuitable (Kim et al., 2016). To address this, a backstepping control with an observer is proposed in (Chen et al., 2016) to estimate state variables

under disturbances for trajectory tracking. A robust adaptive backstepping method to handle parametric uncertainties in the quadrotor's dynamics is presented in (Hua et al., 2018).

Hybrid control techniques demonstrate good performance by combining backstepping and SMC methods. (Jia et al., 2017) proposed a nonlinear controller for path following but lacked an adaptation law, complicating uncertainty estimation. (Shi et al., 2019) introduced a fractional-order controller to reduce chattering, while (Ma et al., 2018) designed a cascade multi-loop controller for finite-time trajectory convergence under wind turbulence.

Various advanced control strategies have been proposed for finite-time convergence in quadrotors. (Muñoz et al., 2017) designed a controller to handle parameter uncertainties and external disturbances in altitude control. (Xue et al., 2021) introduced a complex tracking scheme for moving targets, while (Labbadi et al., 2020) developed a robust approach to enhance speed tracking, precision, and disturbance rejection. However, these controllers involve intricate mathematical formulations and implementation challenges, requiring extensive computational resources for real-world application.

To enhance the advantages of various control methodologies presented in the existing literature and to effectively address the challenges associated with unknown quadrotor parameters, external disturbances, and time-varying loads, this chapter explores the implementation of robust nonlinear control strategies, namely Backstepping, Sliding Mode, and Modified Sliding Mode control techniques, within the MATLAB/Simulink environment. These methods are explored to ensure precise trajectory tracking, position, and attitude stability under external disturbances. Simulations are used to evaluate and compare the performance of these control strategies, contributing to improved quadrotor control for practical applications such as aerial surveillance, reconnaissance, and delivery. The simulation results are compared with existing controllers in the literature across various scenarios.

Section 2 provides an overview of backstepping control. Section 3 introduces sliding mode control. Section 4 explains the design of Modified PID Sliding Mode Control. Simulation results of the proposed control strategies are presented in Section 5. Finally, Section 6 includes conclusions and discussion.

2. Backstepping Control Technique

Backstepping control is a control technique used in aerial robotics, particularly for unmanned aerial vehicles (UAVs) or drones. This technique is a nonlinear control method that ensures the robust and precise control of a drone's

movement. The backstepping approach is based on decomposing the system dynamics into simpler subsystems and designing control laws for each subsystem. This approach has been proven effective in controlling the nonlinear dynamics of drones and ensuring stable and accurate performance. Backstepping control is widely used in applications such as trajectory tracking, altitude control, and position state and orientation stabilization (PhD T. S. Bouabdallah, 2007; S. Bouabdallah & Siegwart, 2005a; Shao et al., 2018).

The backstepping control method is a nonlinear control technique used to regulate the dynamics of complex systems such as drones. The fundamental principle of backstepping is to decompose the complex dynamics of a system into simpler subsystems and design control laws for each of these subsystems. This approach simplifies the control design process by allowing the designer to address the dynamics of each subsystem separately.

The system dynamics of a drone can be decomposed into subsystems, including position state, orientation, altitude, position control, and trajectory tracking. A separate control law can be designed to regulate the dynamics of each subsystem. One of the most significant advantages of the backstepping control approach is its ability to handle the nonlinearities in system dynamics. The control laws designed for each subsystem consider the inherent nonlinearities of the system, ensuring stable and accurate performance. Furthermore, backstepping control provides robust control in the presence of disturbances and uncertainties, making it highly suitable for real-world applications.

In summary, backstepping control is a powerful control technique widely used in the regulation of drones and other aerial robots. Its ability to handle complex system dynamics while providing robust and precise control makes it a prevalent choice for various applications, including autonomous flight, surveillance, and search-and-rescue missions (Alsamhi et al., 2022; Silvagni et al., 2017; Tomic et al., 2012).

2.1. Backstepping Control Design:

In this section, the mathematical model of the quadrotor, as explained and developed in (Y.Nettari, 2023) and rewritten in Eq (1) as follows:

$$\begin{cases} \ddot{x} = \frac{1}{m}\left(\left(C_\phi S_\theta C_\psi + S_\phi S_\psi\right)u_m + d_x\right) - \frac{k_{dx}}{m}\dot{x} \\ \ddot{y} = \frac{1}{m}\left(\left(C_\phi S_\theta S_\psi - S_\phi C_\psi\right)u_m + d_y\right) - \frac{k_{dy}}{m}\dot{y} \\ \ddot{z} = \frac{1}{m}\left(C_\phi C_\theta u_m + d_z\right) - g - \frac{k_{dz}}{m}\dot{z} \\ \ddot{\phi} = \dot{\theta}\dot{\psi}\frac{I_{yy}-I_{zz}}{I_{xx}} - \dot{\theta}\frac{J_r}{I_{xx}}\varpi - \frac{k_{d\Phi}}{I_{xx}}\dot{\phi}^2 + \frac{1}{I_{xx}}u_\Phi + d_\phi \\ \ddot{\theta} = \dot{\phi}\dot{\psi}\frac{I_{zz}-I_{xx}}{I_{yy}} + \dot{\phi}\frac{J_r}{I_{yy}}\varpi - \frac{k_{d\theta}}{I_{yy}}\dot{\theta}^2 + \frac{1}{I_{yy}}u_\Theta + d_\theta \\ \ddot{\psi} = \dot{\phi}\dot{\theta}\frac{I_{xx}-I_{yy}}{I_{zz}} - \frac{k_{d\psi}}{I_{zz}}\dot{\psi}^2 + \frac{1}{I_{zz}}u_\Psi + d_\psi \end{cases} \quad (1a)$$

$$\begin{bmatrix} v_x \\ v_y \\ v_z \end{bmatrix} = \begin{bmatrix} \left(C_\phi S_\theta C_\psi + S_\phi S_\psi\right)\frac{u_m}{m} \\ \left(C_\phi S_\theta S_\psi - S_\phi C_\psi\right)\frac{u_m}{m} \\ \left(C_\phi C_\theta\right)\frac{u_m}{m} - g \end{bmatrix} \quad (1b)$$

a- Altitude Controller:

In this section, the altitude controller for the quadrotor will be explored. First, we define the tracking error signal as shown in the equation below, where z_d denotes the desired altitude signal:

$$e_z = z_d - z \quad (2)$$

Subsequently, the altitude controller is determined as:

$$v_z = \left(\frac{k_{dz}}{m}\dot{z} + c_{z1}\dot{e}_z + \ddot{z}_d + e_z + c_{z2}e_{z1}\right) \quad (3)$$

Where $c_{zi} > 0, i = 1{,}2$ and:

$$e_{z1} = -\dot{z} + c_{z1}e_z + \dot{z}_d \quad (4)$$

Theorem 1: If the control input signal u_m is designed as described above for the altitude dynamics, the error in tracking the desired altitude will asymptotically decrease to zero as time progresses towards infinity.

Proof. Initially, consider the following Lyapunov function.

$$V_{z1} = \frac{1}{2}e_z^2 \quad (5)$$

By combining Equations (2), (4), and (5), we obtain the following:

$$\begin{aligned} \dot{V}_{z1} &= e_z \dot{e}_z \\ &= e_z(\dot{z}_d - \dot{z}) \\ &= e_z(e_{z1} + \dot{z} - c_{z1}e_z - \dot{z}) \\ &= -c_{z1}e_z^2 + e_z e_{z1} \end{aligned} \tag{6}$$

Let us define the following candidate Lyapunov function:

$$V_z = V_{z1} + \frac{1}{2}e_{z1}^2 \tag{7}$$

The time derivative of V_z is given as follows:

$$\dot{V}_z = \dot{V}_{z1} + e_{z1}\dot{e}_{z1} \tag{8}$$

Additionally, by using Equations (4), (6), and the $\ddot{z}$ equation in Eq.(1a), we obtain the following:

$$\begin{aligned} \dot{V}_z &= -c_{z1}e_z^2 + e_z e_{z1} + e_{z1}(-\ddot{z} + c_{z1}\dot{e}_z + \ddot{z}_d) \\ &= -c_{z1}e_z^2 + e_z e_{z1} + e_{z1}\left(-v_z + \frac{K_{dz}}{m}\dot{z} + c_{z1}\dot{e}_z + \ddot{z}_d\right) \end{aligned} \tag{9}$$

By substituting the altitude controller (3) into (9), we obtain,

$$\begin{aligned} \dot{V}_z &= -c_{z1}e_z^2 + e_z e_{z1} + e_{z1}(-e_z - c_{z2}e_{z1}) \\ &= -c_{z1}e_z^2 - c_{z2}e_{z1}^2 \\ &\leq 0 \end{aligned} \tag{10}$$

This concludes the proof, confirming the system's stability.

b- Position Controller:

Likewise, the controllers for X and Y can be expressed as follows:

$$v_x = \frac{k_{dx}}{m}\dot{x} + \ddot{x}_d + c_{x_1}\dot{e}_x + c_{x_2}e_{x_1} + \dot{e}_{x_1} \tag{11}$$

$$v_y = \frac{k_{dy}}{m}\dot{y} + \ddot{y}_d + c_{y_1}\dot{e}_y + c_{y_2}e_{y_1} + \dot{e}_{y_1} \tag{12}$$

Where, $c_{x_1}, c_{x_2}, c_{y_1}, c_{y_2}$ are positive constants that are non-zero, and

$$e_x = x_d - x, \qquad e_{x_1} = -\dot{x} - c_{x_1} e_x + \dot{x}_d$$
$$e_y = y_d - y, \qquad e_{y_1} = -\dot{y} - c_{y_1} e_y + \dot{y}_d$$

c- Attitude Controller:

Similar to the analysis performed for altitude control in the previous section, the design of the attitude controller will be examined in this section. First, the controller for the roll angle will be addressed.

The roll angle tracking error is defined as the difference between the desired roll angle signal, ϕ_d, and the actual ϕ. This is expressed as:

$$e_\phi = \phi_d - \phi \tag{13}$$

The roll controller is then designed as follows:

$$u_\phi = I_{xx}\left(-\dot{\theta}\dot{\psi}\frac{I_{yy}-I_{zz}}{I_{xx}} + \dot{\theta}\frac{J_r}{I_{xx}}\varpi + \frac{k_{d\Phi}}{I_{xx}}\dot{\phi}^2 + \ddot{\phi}_d + c_{\phi 1}\dot{e}_\phi + e_\phi + c_{\phi 2}e_{\phi 1}\right) \tag{14}$$

Where $c_{\phi i} > 0, i = 1{,}2$ and

$$e_{\phi 1} = -\dot{\phi} + c_{\phi 1} e_\phi + \dot{\phi}_d \tag{15}$$

Stability Proof: Consider the following proposed Lyapunov function:

$$V_{\phi 1} = \frac{1}{2} e_\phi^2 \tag{16}$$

The time derivative of $V_{\phi 1}$ is given as follows:

$$\dot{V}_{\phi 1} = e_\phi \dot{e}_\phi \tag{17}$$

By using Equations (13), (15), and (17), we obtain the following:

$$\begin{aligned} \dot{V}_{\phi 1} &= e_\phi \dot{e}_\phi \\ &= e_\phi\left(\dot{\phi}_d - \dot{\phi}\right) \\ &= e_\phi\left(e_{\phi 1} + \dot{\phi} - c_{\phi 1} e_\phi - \dot{\phi}\right) \\ &= -c_{\phi 1} e_\phi^2 + e_\phi e_{\phi 1} \end{aligned} \tag{18}$$

We define the following candidate Lyapunov function:

$$V_\phi = V_{\phi 1} + \frac{1}{2} e_{\phi 1}^2 \tag{19}$$

The time derivative of V_ϕ is given as follows:

$$\dot{V}_\phi = \dot{V}_{\phi 1} + e_{\phi 1} \dot{e}_{\phi 1} \tag{20}$$

By applying equations (15), (18), and the $\ddot{\phi}$ equation from the quadrotor mathematical model to Eq. (20), we obtain the following:

$$\begin{aligned} \dot{V}_\phi &= -c_{\phi 1} e_\phi^2 + e_\phi e_{\phi 1} + e_{\phi 1}\left(-\ddot{\phi} + c_{\phi 1}\dot{e}_\phi + \ddot{\phi}_d\right) \\ &= -c_{\phi 1} e_\phi^2 + e_\phi e_{\phi 1} + e_{\phi 1}\left(-\dot{\theta}\dot{\psi}\frac{I_{yy}-I_{zz}}{I_{xx}} + \dot{\theta}\frac{J_r}{I_{xx}}\varpi + \frac{k_{d\Phi}}{I_{xx}}\dot{\phi}^2 \right. \\ &\qquad \left. -\frac{1}{I_{xx}}u_\Phi + c_{\phi 1}\dot{e}_\phi + \ddot{\phi}_d\right) \end{aligned} \tag{21}$$

By substituting the roll controller (14) into (21), we obtain:

$$\begin{aligned} \dot{V}_\phi &= -c_{\phi 1} e_\phi^2 + e_\phi e_{\phi 1} + e_{\phi 1}\left(-e_\phi - c_{\phi 2} e_{\phi 1}\right) \\ &= -c_{\phi 1} e_\phi^2 - c_{\phi 2} e_{\phi 1}^2 \\ &\leq 0 \end{aligned} \tag{22}$$

Similarly, as what we have done above with the roll controller, we can formulate the controllers for pitch and yaw as follows:

$$u_\theta = I_{yy}\left(-\dot{\phi}\dot{\psi}\frac{I_{zz}-I_{xx}}{I_{yy}} - \dot{\phi}\frac{J_r}{I_{yy}}\varpi + \frac{k_{d\theta}}{I_{yy}}\dot{\theta}^2 + \ddot{\theta}_d + c_{\theta 1}\dot{e}_\theta + e_\theta + c_{\theta 2} e_{\theta 1}\right) \tag{23}$$

$$u_\psi = I_{zz}\left(-\dot{\phi}\dot{\theta}\frac{I_{xx}-I_{yy}}{I_{zz}} + \frac{k_{d\Psi}}{I_{zz}}\dot{\psi}^2 + \ddot{\psi}_d + c_{\psi 1}\dot{e}_\psi + e_\psi + c_{\psi 2} e_{\psi 1}\right) \tag{24}$$

Where, $c_{\Theta_1}, c_{\Theta_2}, c_{\psi_1}, c_{\psi_2}$ are positive constants that are non-zero, and;

$$e_\Theta = \Theta_d - \Theta\,, \qquad e_{\Theta_1} = -\dot{\Theta} - c_{\Theta_1} e_\Theta + \dot{\Theta}_d$$
$$e_\psi = \psi_d - \psi\,, \qquad e_{\psi_1} = -\dot{\psi} - c_{\psi_1} e_\psi + \dot{\psi}_d$$

Similarly, the stability proof for the pitch and yaw angle controllers can be conducted in the same way as for the roll angle.

3. Sliding Mode Control Technique

This section explores the core principles of control theory using classical sliding modes. For a more in-depth discussion, readers can refer to the works of (X. Liu et al., 1999; Perruquetti & Barbot, 2002; Slotine & Li, 1991; V. Utkin et al., 2017; V. I. Utkin, 2013). Sliding Mode Control (SMC) is a robust control strategy designed to guide system trajectories toward a predefined sliding surface in the state space and ensure their confinement within a finite time. This surface encapsulates the desired system dynamics, serving as a reference for system behavior. The design process of an SMC law comprises two fundamental stages: first, the formulation of an appropriate sliding surface that characterizes the intended system response, and second, the development of a discontinuous control law capable of driving system trajectories toward this surface while guaranteeing their persistence, even in the presence of uncertainties and external disturbances.

3.1 Synthesis of the Sliding Surface:

The primary control objective is to make the state vector $x(t)$ follow the desired trajectory $x_d(t)$, To achieve this, the sliding surface is synthesized using the sliding variable, defined as:

$$s(t) = [s_1(t), \quad s_2(t), \quad s_3(t), \quad \dots, \quad s_n(t)]^T \tag{25}$$

Where, $s_i(t)|_{i=1,n}$ are system-dependent functions that act as virtual outputs. These functions contribute to reducing the tracking error and guiding the system toward the desired behavior.

Definition 1 (Perruquetti & Barbot, 2002): If the solution of the system exists such that $s(t) = 0$ for all $t \geq T_c$ there is an ideal sliding mode with a finite time T_c.

As the system trajectories move along the sliding surface (see Figure.1), the dynamics reduce to a lower-order system, with a degree one less than the system's relative degree.

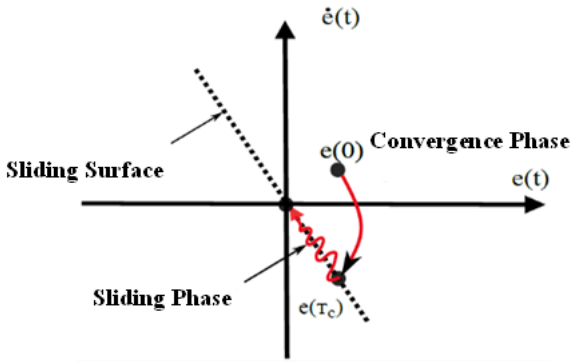

Figure 1: Sliding Mode Control Phase Plane

The reduced dynamics are defined by a linear sliding surface through the origin, which exponentially converges to the origin if stable. For sliding mode, the surface's relative degree must be 1. This linear sliding surface is expressed as bellow, where r is equal to 2, and $\mathfrak{h} \epsilon \mathbb{R}^{nXn}$ is a diagonal matrix and $s(t)$ is a Hurwitz polynomial as shown in (Perruquetti & Barbot, 2002; V. I. Utkin, 2013):

$$s(t) = \left(\frac{d}{dt} + \mathfrak{h}\right)^{r-1} e(t) \tag{26}$$

As the sliding surface approaches zero, the tracking error $e(t)$ asymptotically converges with dynamics set by matrix $\mathfrak{h}$. The relative degree condition holds if $u(t)$ appears in $e^r(t)$ after differentiating $s(t)$.

3.2 Sliding Mode Control Design

To effectively design SMC control, the surface function must be properly maintained by satisfying the attractiveness condition $s(t) = 0$ as shown in (V. Utkin et al., 2017). We choose the following Lyapunov function:

$$V = \frac{1}{2} s(t)^T s(t) \tag{27}$$

This function is defined as positive definite for all $\forall\ s(t) \neq 0$. For the sliding surface to reach zero, the Lyapunov function's derivative $\dot{V} = s(t)^T \dot{s}(t)$ must be negative:

This condition alone does not ensure finite-time convergence, requiring a stronger criterion. In SMC, this is the nonlinear K-attractivity condition (V. I. Utkin, 1977).

$$s_i(t)\,\dot{s}_i(t) \le -K_i|s_i(t)|, \qquad K_i > 0|_{i=1,\dots,n} \tag{28}$$

In other terms, it reduces to making the following selection:

$$\dot{s}(t) = -K\text{sign}(s(t)) \tag{29}$$

Where $K = \text{diag}(K_1, K_2, \dots, K_n)$ is a diagonal matrix with strictly positive elements, $[\text{sign}(s_1(t)), \dots, \text{sign}(s_n(t))]^T$, and

$$\text{sign}(s(t)) = \begin{cases} 1, & \text{if } s(t) > 0 \\ 0, & \text{if } s(t)0 = 0 \\ -1, & \text{if } s(t)0 < 0 \end{cases} \tag{30}$$

By using this convergence law, $s_i(t)|_{i=1,\dots,n}$, reaches zero in finite time, bounded by $T_{c,i}$ shown in Eq. (31), where $s_i(0)$ is the initial sliding surface value.

$$T_{c,i} \le \frac{|s_i(0)|}{K_i} \tag{31}$$

Without considering uncertainties, $\dot{s}_i(t)$ is given by:

$$\begin{aligned} \dot{s}(t) &= \frac{\partial s(t)}{\partial x(t)}\frac{\partial x(t)}{\partial t} = \frac{\partial s(t)}{\partial x(t)}\dot{x}(t) \\ &= \frac{\partial s(t)}{\partial x(t)}[\mathcal{F}(x(t)) + \mathcal{G}(x(t))u(t)] \end{aligned} \tag{32}$$

By using the previous equation and solving $\dot{s}(t) = -\text{sign}\big(s(t)\big)$, we derive the Sliding Mode Control law as given in Eq. (33) below:

$$u(t) = -\Xi^{-1}\frac{\partial s(t)}{\partial x(t)}\mathcal{F}\big(x(t)\big) - \Xi^{-1}K\ \text{sign}(s(t)) \tag{33}$$

This control is only available if $\Xi = \frac{\partial s(t)}{\partial x(t)}\mathcal{G}(x(t))$ matrix is invertible. Note that the control law in equation (33) consists of two parts:

$$u_{eq}(t) = -\Xi^{-1}\frac{\partial s(t)}{\partial x(t)}\mathcal{F}(x(t)) \tag{34a}$$

$$u_{\text{dis}}(t) = -\Xi^{-1}K\ \text{sign}(s(t)) \tag{34b}$$

The control input $u(t)$ consists of two components. The first, $u_{eq}\ (t)$, is continuous and known as the equivalent control, governing the sliding phase for $t \in [T_{ci}, \infty]$ where system trajectories remain on the sliding surface. During this phase, system behavior is entirely dictated by the sliding surface. The second component, $u_{dis}\ (t)$, is discontinuous and manages the reaching phase for $t \in [0, T_{ci}]$, where trajectories move toward the sliding surface. The convergence time depends on the choice of matrix K; larger K values result in faster convergence. Various discontinuous control structures exist in the literature, with one of the most common being the constant gain convergence law.

$$\dot{s}(t) = -K\ \text{sign}(s(t)) \tag{35}$$

This method simplifies control law synthesis where K is a diagonal matrix composed of positive definite constants. However, low gains cause slow convergence, while high gains cause chattering problem.

A linear state feedback convergence law:

$$\dot{s}(t) = -K_1 s(t) - K_2 \text{sign}(s(t)) \tag{36}$$

Where K_1 ve K_2, are diagonal matrices with positive definite gains, this law ensures fast convergence for large $s(t)$, following an exponential convergence principle:

$$\dot{s}(t) = -K(s(t))\text{sign}(s(t)) \tag{37}$$

Where $K(s(t)) = \text{diag}\left(\frac{K_1}{\mathcal{N}_1 s_1(t)}, , \frac{K_n}{\mathcal{N}_n s_n(t)}\right)$ and $K_i > 0 =|_{i=1,,n}$, and the term $\mathcal{N}_i(s_i(t))$ is defined in (S. V. Emeryanov et al., 1996).

4. PID Sliding Mode Control Technique

The previous section shows that the sliding mode approach features a simple and flexible design. In this section, we integrate a proportional, derivative, and integral of the tracking error actions into the sliding surfaces to eliminate steady-state error, providing robustness against disturbances and model uncertainties (Perruquetti & Barbot, 2002). The outer-loop the proposed PIDSMC controllers generate (v_x, v_y, v_z) control signals for the desired position state, attitude (Φ_d, Θ_d), and total thrust u_m, while the inner-loop PIDSMC

controllers stabilize the quadrotor by controlling roll, pitch, and yaw torques. This approach also addresses dual disturbances $d_i(t)$.

To improve performance, the PIDSMC method extends classical PID control by designing sliding surfaces based on position and velocity dynamics. Using the mathematical model developed in (Y.Nettari, 2023) and rewritten in the Eq. (38) below.

$$\begin{cases} \dot{\mathcal{X}}_1 = \mathcal{X}_2 \\ \dot{\mathcal{X}}_3 = \mathcal{X}_4 \\ \dot{\mathcal{X}}_5 = \mathcal{X}_6 \\ \dot{\mathcal{X}}_2 = \rho_{1\Phi}\mathcal{X}_4\mathcal{X}_6 + \rho_{2\Phi}\mathcal{X}_4 + \rho_{3\Phi}\mathcal{X}_2^2 + \rho_1 u_\Phi + d_\Phi \\ \dot{\mathcal{X}}_4 = \rho_{1\Theta}\mathcal{X}_2\mathcal{X}_6 + \rho_{2\Theta}\mathcal{X}_2 + \rho_{3\Theta}\mathcal{X}_4^2 + \rho_2 u_\Theta + d_\Theta \\ \dot{\mathcal{X}}_6 = \rho_{1\Psi}\mathcal{X}_2\mathcal{X}_4 + \rho_{2\Psi}\mathcal{X}_6^2 + \rho_3 u_\Psi + d_\Psi \\ \dot{\mathcal{X}}_7 = \mathcal{X}_8 \\ \dot{\mathcal{X}}_9 = \mathcal{X}_{10} \\ \dot{\mathcal{X}}_{11} = \mathcal{X}_{12} \\ \dot{\mathcal{X}}_8 = \rho_X\mathcal{X}_8 + \frac{1}{m}\left(C_{\mathcal{X}_1}S_{\mathcal{X}_3}C_{\mathcal{X}_5} + S_{\mathcal{X}_1}S_{\mathcal{X}_5}\right)u_m + d_x \\ \dot{\mathcal{X}}_{10} = \rho_Y\mathcal{X}_{10} + \frac{1}{m}\left(C_{\mathcal{X}_1}S_{\mathcal{X}_3}S_{\mathcal{X}_5} - S_{\mathcal{X}_1}C_{\mathcal{X}_5}\right)u_m + d_y \\ \dot{\mathcal{X}}_{12} = \rho_Z\mathcal{X}_{12} - g + \frac{1}{m}\left(C_{\mathcal{X}_1}C_{\mathcal{X}_3}\right)u_m + d_z \end{cases} \tag{38}$$

where:

$$\rho_{1\Phi} = \frac{(I_{yy} - I_{zz})}{I_{xx}}, \rho_{2\Phi} = \frac{-\varpi J_r}{I_{xx}}, \rho_{3\Phi} = \frac{-K_{d\Phi}}{I_{xx}}, \rho_{1\Theta} = \frac{(I_{zz} - I_{xx})}{I_{yy}}, \rho_{2\Theta} = \frac{\varpi J_r}{I_{yy}}, \rho_{3\Theta} = \frac{-K_{d\Theta}}{I_{yy}}, \rho_{1\Psi} = \frac{(I_{xx} - I_{yy})}{I_{zz}}$$
$$\rho_{2\Psi} = \frac{-K_{d\Psi}}{I_{zz}}, \rho_X = \frac{-K_{dx}}{m}, \rho_Y = \frac{-K_{dy}}{m}, \rho_Z = -\frac{K_{dz}}{m}, \rho_1 = \frac{1}{I_{xx}}, \rho_2 = \frac{1}{I_{yy}}, \text{ and } \rho_3 = \frac{1}{I_{zz}}$$

The tracking errors for the position subsystems are expressed as shown in Eq. (39a) and attitude subsystems are expressed as shown in Eq. (39b):

$$\begin{bmatrix} e_1(t) \\ e_3(t) \\ e_5(t) \end{bmatrix} = \begin{bmatrix} \mathcal{X}_1 - \Phi_d \\ \mathcal{X}_3 - \Theta_d \\ \mathcal{X}_5 - \Psi_d \end{bmatrix}, \qquad \begin{bmatrix} e_2(t) \\ e_4(t) \\ e_6(t) \end{bmatrix} = \begin{bmatrix} \mathcal{X}_2 - \dot{\Phi}_d \\ \mathcal{X}_4 - \dot{\Theta}_d \\ \mathcal{X}_6 - \dot{\Psi}_d \end{bmatrix} \tag{39a}$$

$$\begin{bmatrix} e_7(t) \\ e_9(t) \\ e_{11}(t) \end{bmatrix} = \begin{bmatrix} \mathcal{X}_7 - x_d \\ \mathcal{X}_9 - y_d \\ \mathcal{X}_{11} - y_d \end{bmatrix}, \qquad \begin{bmatrix} e_8(t) \\ e_{10}(t) \\ e_{12}(t) \end{bmatrix} = \begin{bmatrix} \mathcal{X}_8 - \dot{x}_d \\ \mathcal{X}_{10} - \dot{y}_d \\ \mathcal{X}_{12} - \dot{z}_d \end{bmatrix} \tag{39b}$$

The PID sliding surfaces have been selected as follows:

$$\begin{cases} s_1(t) = K_{p\Phi} e_1(t) + K_{i\Phi} \int e_1(t)dt + K_{d\Phi} \dot{e}_1(t) \\ s_3(t) = K_{p\Theta} e_3(t) + K_{i\Theta} \int e_3(t)dt + K_{d\Theta} \dot{e}_3(t) \\ s_5(t) = K_{p\Psi} e_5(t) + K_{i\Psi} \int e_5(t)dt + K_{d\Psi} \dot{e}_5(t) \end{cases} \quad (40a)$$

$$\begin{cases} s_7(t) = K_{px} e_7(t) + K_{ix} \int e_7(t)dt + K_{dx} \dot{e}_7(t) \\ s_9(t) = K_{py} e_9(t) + K_{iy} \int e_9(t)dt + K_{dy} \dot{e}_9(t) \\ s_{11}(t) = K_{pz} e_{11}(t) + K_{iz} \int e_{11}(t)dt + K_{dz} \dot{e}_{11}(t) \end{cases} \quad (40b)$$

$K_{pj}, K_{ij}, K_{dj}\big|_{j=(\Phi,\Theta,\Psi,x,y,z)} > 0.$

The time derivative of the surfaces in the proposed approach is expressed as follows:

$$\begin{cases} \dot{s}_1(t) = K_{p\Phi} \dot{e}_1(t) + K_{i\Phi} e_1(t) + K_{d\Phi} \ddot{e}_1(t) \\ \dot{s}_3(t) = K_{p\Theta} \dot{e}_3(t) + K_{i\Theta} e_3(t) + K_{d\Theta} \ddot{e}_3(t) \\ \dot{s}_5(t) = K_{p\Psi} \dot{e}_5(t) + K_{i\Psi} e_5(t) + K_{d\Psi} \ddot{e}_5(t) \end{cases} \quad (41a)$$

$$\begin{cases} \dot{s}_7(t) = K_{px} \dot{e}_7(t) + K_{ix} e_7(t) + K_{dx} \ddot{e}_7(t) \\ \dot{s}_9(t) = K_{py} \dot{e}_9(t) + K_{iy} e_9(t) + K_{dy} \ddot{e}_9(t) \\ \dot{s}_{11}(t) = K_{pz} \dot{e}_{11}(t) + K_{iz} e_{11}(t) + K_{dz} \ddot{e}_{11}(t) \end{cases} \quad (41b)$$

The switching control laws are given as follows:

$$\dot{s}(t) = -K_s sign(s(t)) \quad (42)$$

Where $K_s > 0$ and the ***sign*** function is discontinuous, the following equations express the switching control laws for the translational and rotational subsystems.

$$\begin{cases} \dot{s}_1(t) = -K_1 sign(s_1(t)) \\ \dot{s}_3(t) = -K_3 sign(s_3(t)), \\ \dot{s}_5(t) = -K_5 sign(s_5(t)) \end{cases} \quad \begin{cases} \dot{s}_7(t) = -K_7 sign(s_7(t)) \\ \dot{s}_9(t) = -K_9 sign(s_9(t)) \\ \dot{s}_{11}(t) = -K_{11} sign(s_{11}(t)) \end{cases} \quad (43)$$

By using (41b) and (43), we obtain the position loop's virtual control as follows:

$$\begin{aligned} v_x &= \rho_X \mathcal{X}_8 - d_x + \ddot{x}_d - \frac{1}{K_{dx}}\left(K_{px}\dot{e}_7(t) + K_{ix}e_7(t) + K_{s7}sign(s_7(t))\right) \\ v_y &= \rho_Y \mathcal{X}_{10} - d_y + \ddot{y}_d - \frac{1}{K_{dy}}\left(K_{py}\dot{e}_9 + K_{iy}e_9(t) + K_{s9}sign(s_9(t))\right) \\ v_z &= \rho_Z \mathcal{X}_{12} - d_z + \ddot{z}_d - \frac{1}{K_{dz}}\left(K_{pz}\dot{e}_{11}(t) + K_{iz}e_{11}(t) + K_{s11}sign(s_{11}(t))\right) \end{aligned} \tag{44}$$

Similarly, the control signals for the inner loop can be easily derived from equations (41a) and (43).

$$\begin{aligned} u_\Phi &= \frac{1}{\rho_1}\left(-\rho_{1\Phi}\mathcal{X}_4\mathcal{X}_6 - \rho_{2\Phi}\mathcal{X}_4 - \rho_{3\Phi}\mathcal{X}_2^2 - d_\Phi + \ddot{\Phi}_d - \frac{1}{K_{d\Phi}}\left(K_{p\Phi}\dot{e}_1(t) + K_{i\Phi}e_1(t) + K_{s1}\text{sign}(s_1)\right)\right) \\ u_\Theta &= \frac{1}{\rho_2}\left(-\rho_{1\Theta}\mathcal{X}_2\mathcal{X}_6 - \rho_{2\Theta}\mathcal{X}_2 - \rho_{3\Theta}\mathcal{X}_4^2 - d_\Theta + \ddot{\Theta}_d - \frac{1}{K_{d\Theta}}\left(K_{p\Theta}\dot{e}_3(t) + K_{i\Theta}e_3(t) + K_{s_3}\text{sign}(s_3)\right)\right) \\ u_\Psi &= \frac{1}{\rho_3}\left(-\rho_{1\Psi}\mathcal{X}_2\mathcal{X}_4 - \rho_{2\Psi}\mathcal{X}_6^2 - d_\Psi + \ddot{\Psi}_d - \frac{1}{K_{d\Psi}}\left(K_{p\Psi}\dot{e}_5(t)K_{i\Psi}e_5(t) + K_{s_5}\text{sign}(s_5)\right)\right) \end{aligned} \tag{45}$$

Where $K_{si}|_{i=(x,y,z,\Phi,\Theta,\Psi)} > 0$.

Theorem 1. For the x sub-system controlled by v_x, it can be concluded that the subsystem remains stable.

Proof 1. The x sub-system's Lyapunov function is:

$$V_7 = \frac{1}{2}s_7(t)^2 \tag{46}$$

Where $V_7(0) = 0$ and for $s_7(t) \neq 0$, $V_7(t) > 0$. The time derivative of V_7 is given as follows:

$$\dot{V}_7 = s_7(t)\dot{s}_7(t) \tag{47}$$

By using Eq. (41), the equation (47) transforms into the following form:

$$\dot{V}_7 = s_7(t)\left(K_{px}\dot{e}_7(t) + K_{ix}e_7(t) + K_{dx}\ddot{e}_7(t)\right) \tag{48}$$

Substituting the second time derivative of $e(t)$ into (48), we obtain:

$$\dot{V}_7 = s_7(t)\left(K_{px}\dot{e}_7(t) + K_{ix}e_7(t) + K_{dx}(-\ddot{x}_d - \rho_X\mathcal{X}_8 + d_x + v_x)\right) \tag{49}$$

By substituting the v_x control law given in (44), we obtain the following:

$$\dot{V}_7 = s_7(t)\Big(K_{px}\dot{e}_7 + K_{ix}e_7(t) + K_{dx}\big(-\ddot{x}_d - \rho_X \mathcal{X}_8 + d_x + \rho_X \mathcal{X}_8 - d_x + \ddot{x}_d - \frac{1}{K_{dx}}\big(K_{px}\dot{e}_7 + K_{ix}e_7(t) + K_{s7}\text{sign}(s_7(t))\big)\big)\Big) \quad (50)$$

After a straightforward calculation, we obtain:

$$\begin{aligned}\dot{V}_7 &= -s_7(t)\frac{K_{s7}}{K_{dx}}sign(s_7(t)) \\ &= -\frac{K_{s7}}{K_{dx}}|s_7(t)| \le 0\end{aligned} \quad (51)$$

Since the Eq. (51) is less than zero, then the x sub-system is stable. Although PIDSMC is robust against disturbances, it may cause chattering—high-frequency oscillations in steady-state due to model errors, numerical noise, or measurement noise.

This can lead to higher energy consumption and rotor damage, potentially causing system failure. Saturation functions are often used to reduce chattering in PIDSMC, providing practical stability in the closed-loop system, as shown in Figure 2. The hyperbolic tangent function $sign\, s(t) = tanh(\frac{s(t)}{\zeta})$ is used instead of the sign function.

In practice, ζ should be small enough to balance chattering reduction and acceptable steady-state error.

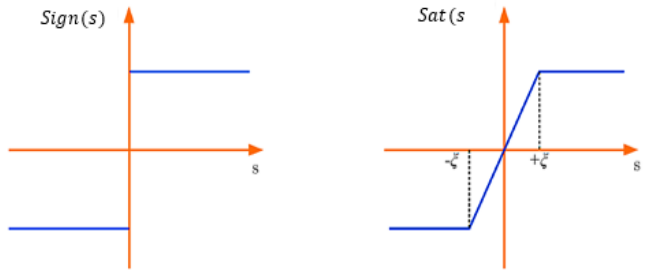

Figure 2: Linear saturation function approximation of the sign function.

5. Simulation Results

Numerical simulations in two scenarios with Basic SMC, Backstepping Control (BsC), and PID Sliding Mode Control (PIDSMC) are used to assess the proposed control laws under both constant and time-varying disturbances, highlighting and exposing the advantages and disadvantages of each technique.

5.1 Scenario 1: Under Constant Disturbances

This analysis assesses the robustness and effectiveness of the proposed control method. By examining simulation results of SMC, BsC, and PIDSMC in tracking the quadrotor's desired trajectory, we can identify the benefits each technique offers to the system.

As we know, the sliding mode controller is highly robust against external disturbances and model uncertainties, as it utilizes the sliding mode surface to direct the system toward the desired equilibrium state and ensure stability. Backstepping control has the capability to handle complex nonlinear systems and provide high-performance control. The PIDSMC method combines the robustness and fast response of sliding mode control with the adaptability and ease of implementation of PID control, making it particularly effective in applications involving complex nonlinear systems and significant disturbances.

This scenario examines the performance of SMC, BsC, and PIDSMC strategies under constant external disturbances and identifies the most effective approach.

The proposed constant external disturbance expressions are as follows:

$$d_x = \begin{cases} 0\ m/s^2 & t \in [0,5) \\ 1\ m/s^2 & t \in [5,40] \end{cases}, \quad d_y = \begin{cases} 0\ m/s^2 & t \in [0,15) \\ 1\ m/s^2 & t \in [15,40] \end{cases}, \quad d_z = \begin{cases} 0\ m/s^2 & t \in [0,25) \\ 1\ m/s^2 & t \in [25,40] \end{cases} \tag{52}$$

$$d_\Phi = \begin{cases} 0\ rad/s^2 & t \in [0,10) \\ 1\ rad/s^2 & t \in [10,40] \end{cases}, \quad d_\theta = \begin{cases} 0\ rad/s^2 & t \in [0,20) \\ 1\ rad/s^2 & t \in [20,40] \end{cases}, \quad d_\psi = \begin{cases} 0\ rad/s^2 & t \in [0,30) \\ 1\ rad/s^2 & t \in [30,40] \end{cases} \tag{53}$$

The vehicle's initial conditions are the position $[x_d, y_d, z_d] = [0,0,0]\ m$ and the attitude angles $[\Phi_d, \Theta_d, \psi_d\ ] = [0,0,0.5]\ rad$. The reference trajectory in this scenario includes different segment types, as detailed below:

$$x_d = \begin{cases} 0.5cos(0.5t)m & t \in [0,4\pi) \\ 0.5m & t \in [4\pi,20) \\ 0.25t - 4.5m & t \in [20,30) \\ 3m & t \in [30,80] \end{cases} \quad y_d = \begin{cases} 0.5sin(0.5t)m & t \in [0,4\pi) \\ 0.25t - 3.14m & t \in [4\pi,20) \\ 5 - \pi m & t \in [20,30) \\ -0.2358t + 8.94m & t \in [30,40] \\ -0.5m & t \in [40,80] \end{cases} \tag{54}$$

$$z_d = \begin{cases} 0.125t + 1m & t \in [0,4\pi) \\ 0.5\pi + 1m & t \in [4\pi,40) \\ exp(-0.2t + 8.944)m & t \in [40,80) \end{cases} \Psi_d = \begin{cases} \frac{\pi}{4} rad & t \in [0,50) \\ 0rad & t \in (50,80] \end{cases} \tag{55}$$

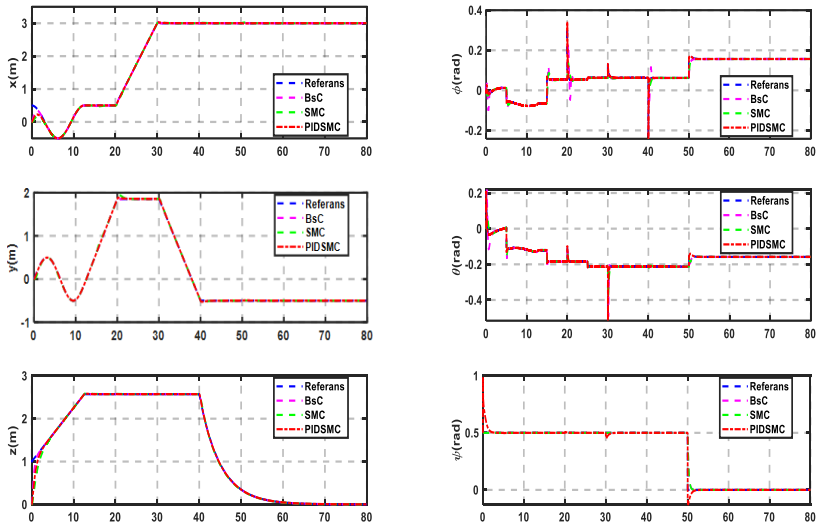

a) Position (x, y, z) **b)** Attitude (ϕ, θ, ψ)

Figure 3 Scenario 1: System time responses of SMC, BsC, and PIDSMC.

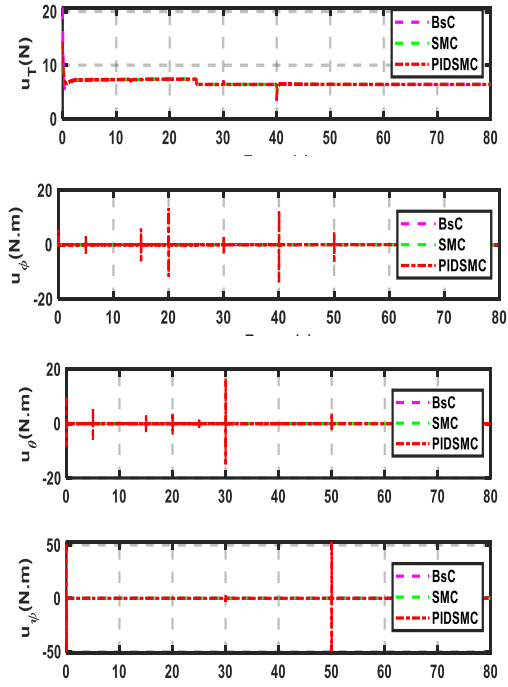

Figure 4 Scenario 1: Control input signals of SMC, BsC, and PIDSMC

controllers

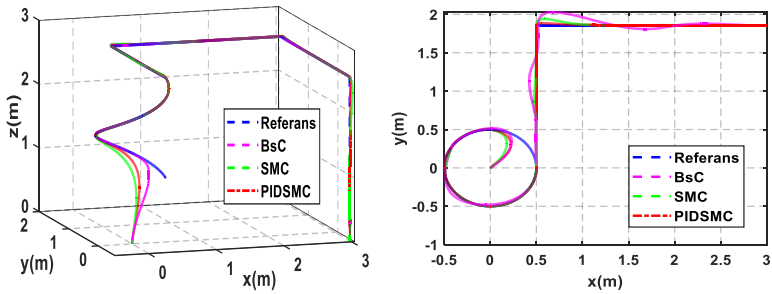

Figure 5 Scenario 1: 3D trajectory tracking of the quadrotor drone

The simulation results of our proposed controller are compared with the backstepping and sliding mode controllers proposed by T. Huang et al. and A. Noordin et al., as shown in Figures 3–5 (Noordin et al., 2019; Perruquetti & Barbot, 2002). These figures illustrate that when constant disturbances are introduced to the quadrotor drone system, along with abrupt adjustments to the desired flight trajectory, our PIDSMC developed control strategy demonstrates exceptional robustness in maintaining trajectory tracking. It guarantees stable tracking in the presence of external disturbances. Also, it delivers quick response times, effectively adjusting to aggressive maneuvers while keeping the trajectory deviation minimal from the desired path.

The figures show that PIDSMC outperforms BsC and SMC. Figure 3a demonstrates that PIDSMC accurately tracks the desired position and remains stable, while SMC responds more slowly during transitions. Figure 3b highlights the attitude performance, where roll, pitch, and yaw angles quickly follow reference values, ensuring stable quadrotor control. Figure 4 displays the total thrust u_m and the three rotational torques $(u_\Phi, u_\Theta, u_\Psi)$, showing that PIDSMC produces smoother, lower-amplitude control inputs with minimal chattering.

Finally, Figure 5 presents the 3D trajectory tracking results. It can be observed that the PIDSMC control strategy enables the quadrotor drone to follow the desired trajectory, even from an initial position far from the desired location. The proposed controller exhibits better tracking performance during transition phases compared to the backstepping and SMC techniques (see Figure 5).

5.2 Scenario 2: Under Time-Varying Disturbances

This scenario examines time-varying disturbances, including external factors and wind gusts, that influence the quadrotor's position and attitude $(\Phi, \Theta, \Psi, x, y, z)$. The disturbances affecting the six degrees of freedom are

represented as: $d_i|_{(i=\Phi,\Theta,\Psi,x,y,z)} = 0.5\,cos(t)$. The initial conditions for the six degrees of freedom are set to: $[0.5, 0.5, 1]\,m$ and $[0\ 0\ 0{,}5]\,rad$. For this scenario, the desired trajectory used is described by the following equations:

$$x_d = cos(t) + 1m, y_d = sin(t) + 1m, z_d = 0.5t + 1m,$$
$$\Psi_d = 0.5sin(t)rad \tag{56}$$

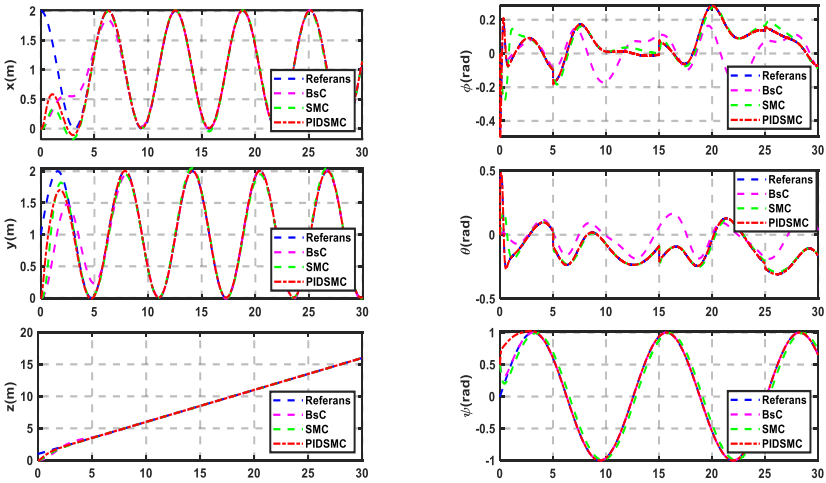

a) Quadrotor Position (x, y, z) **b)** Quadrotor Attitude (ϕ, θ, ψ)

Figure 6 Scenario 2: System Time Responses (SMC, BsC, and PIDSMC)

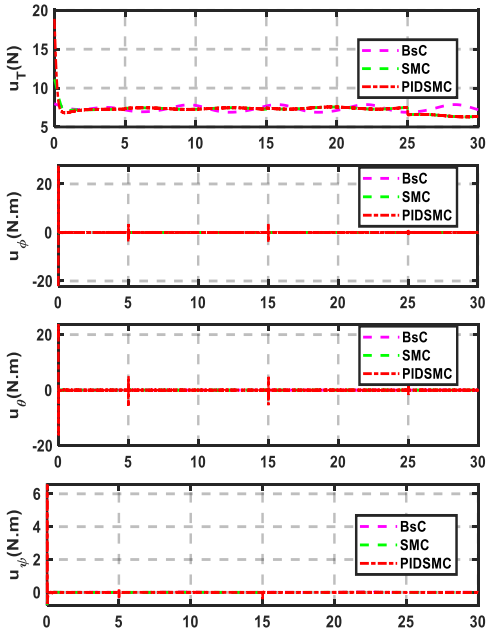

Figure 7 Scenario 2: Control Input Signals of SMC, BsC, and PIDSMC Controllers

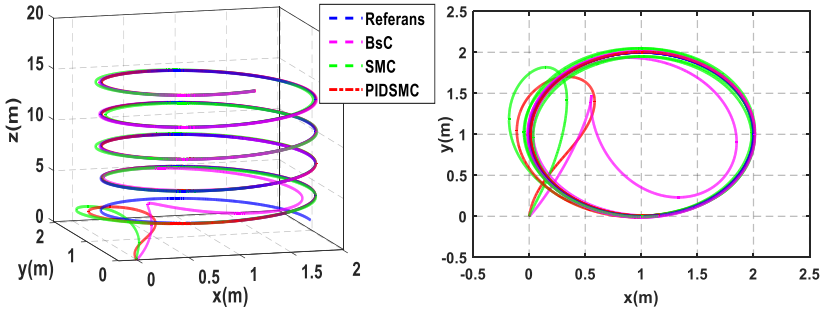

Figure 8 Scenario 2: 3D Trajectory Tracking of the Quadrotor Drone

The simulation results and performance comparisons of the proposed PIDSMC approach with Sliding Mode Control (SMC) and Backstepping Control (BsC) techniques are presented in Figures 6–8. To enhance the robustness of the SMC and BsC controllers, a modified robust controller (PIDSMC) has been proposed. This controller effectively mitigates the impact of disturbances on the quadrotor drone, thereby improving overall robustness. From the results presented in Figures 6–8, it is evident that the performance of the proposed controller surpasses that of Backstepping Control and Sliding Mode Control (SMC), as introduced in Sections 2 and 3, and developed in the work of S. Bouabdallah et al. (S. Bouabdallah & Siegwart, 2005a). In Figure 6a, which illustrates the position control performance, we observe that the proposed PIDSMC strategy enables the quadrotor drone to track the desired trajectory in a short time. Figure 6b presents the attitude response in terms of pitch, roll, and yaw angles, where the yaw angle is shown to precisely follow the desired sinusoidal reference. Despite the presence of time-varying disturbances and changes in the desired trajectory, the Euler angles (Φ, θ) remain closely aligned with their original reference values.

The control input signals of the quadrotor drone system are presented in Figure 7. These control inputs exhibit smoother and higher-quality responses compared to Sliding Mode Control (SMC) and Backstepping Control (BsC) methods. Figure 7 illustrates that the PIDSMC method effectively mitigates the chattering issue caused by discontinuous control elements in the SMC and BsC techniques. Additionally, it enhances transient response and overall robustness. The 3D flight trajectory is depicted in Figure 8. Based on these observations, the proposed controller demonstrates superior tracking performance for circular trajectories, even under time-varying external disturbances.

Ultimately, the results from both Scenario 1 and Scenario 2, the system outcomes distinctly demonstrate the variations between SMC, BsC, and the proposed PIDSMC approach, especially during transient phase. For instance,

Figures 3a and 6a illustrate that the proposed method achieves superior trajectory tracking performance during the transient and steady state phases.

6. Conclusion

This chapter analyzed the performance of Sliding Mode Control (SMC), Backstepping Control (BsC), and PID-based Sliding Mode Control (PIDSMC) for quadrotor trajectory tracking under constant and time-varying disturbances. Numerical simulations clearly demonstrated the superior performance of PIDSMC over the other methods.

In Scenario 1, under constant disturbances, PIDSMC exhibited exceptional robustness and tracking accuracy, significantly outperforming SMC and BsC. While SMC maintained robustness but suffered from slow transitions, and BsC managed nonlinearities but lacked disturbance rejection, PIDSMC effectively combined these strengths. It ensured rapid response, minimized tracking error, and reduced chattering, leading to more stable and precise control.

Scenario 2 further reinforced PIDSMC's advantages in handling time-varying disturbances. It consistently maintained precise trajectory tracking despite dynamic external influences. Compared to SMC and BsC, PIDSMC exhibited superior disturbance rejection, faster convergence, and enhanced transient response, making it the most effective strategy for real-world quadrotor applications.

Overall, PIDSMC not only integrates the robustness of SMC with the adaptability of PID but also offers smoother control inputs, improved stability, and superior trajectory tracking under diverse operating conditions. Its ability to handle complex disturbances while maintaining precision and efficiency makes it a highly promising approach for advanced UAV control. Future work may focus on further optimization and experimental validation to solidify its practical applicability.

References

Aguilar-Ibáñez, C., Sira-Ramírez, H., Suárez-Castañón, M. S., Martínez-Navarro, E., & Moreno-Armendariz, M. A. (2012). The trajectory tracking problem for an unmanned four-rotor system: Flatness-based approach. *International Journal of Control*, *85*(1), 69–77. https://doi.org/10.1080/00207179.2011.638328

Ai, X., & Yu, J. (2019). Fixed-time trajectory tracking for a quadrotor with external disturbances: A flatness-based sliding mode control approach. *Aerospace Science and Technology*, *89*, 58–76. https://doi.org/10.1016/j.ast.2019.03.059

Alexis, K., Nikolakopoulos, G., & Tzes, A. (2014). On trajectory tracking model predictive control of an unmanned quadrotor helicopter subject to aerodynamic disturbances. *Asian Journal of Control*, *16*(1), 209–224. https://doi.org/10.1002/asjc.587

Alsamhi, S. H., Shvetsov, A. V., Kumar, S., Shvetsova, S. V., Alhartomi, M. A., Hawbani, A., Rajput, N. S., Srivastava, S., Saif, A., & Nyangaresi, V. O. (2022). UAV Computing-Assisted Search and Rescue Mission Framework for Disaster and Harsh Environment Mitigation. *Drones*, *6*(7). https://doi.org/10.3390/drones6070154

Altuğ, E., Ostrowski, J. P., & Taylor, C. J. (2005). Control of a quadrotor helicopter using dual camera visual feedback. *International Journal of Robotics Research*, *24*(5), 329–341. https://doi.org/10.1177/0278364905053804

Ansari, U., Bajodah, A. H., & Hamayun, M. T. (2019). Quadrotor Control Via Robust Generalized Dynamic Inversion and Adaptive Non-Singular Terminal Sliding Mode. *Asian Journal of Control*, *21*(3), 1237–1249. https://doi.org/10.1002/asjc.1800

Antonelli, G., Cataldi, E., Arrichiello, F., Giordano, P. R., Chiaverini, S., & Franchi, A. (2018). Adaptive Trajectory Tracking for Quadrotor MAVs in Presence of Parameter Uncertainties and External Disturbances. *IEEE Transactions on Control Systems Technology*, *26*(1), 248–254. https://doi.org/10.1109/TCST.2017.2650679

Bouabdallah, S., Murrieri, P., & Siegwart, R. (2004). *Design and Control of an Indoor Micro Quadrotor*. www.aerovironment.com

Bouabdallah, S., Noth, A., & Siegwart, R. (2004). PID vs LQ control techniques applied to an indoor micro Quadrotor. *2004 IEEE/RSJ International Conference on Intelligent Robots and Systems (IROS)*, *3*, 2451–2456. https://doi.org/10.1109/iros.2004.1389776

Bouabdallah, S. (PhD T. (2007). design and control of quadrotors with application to autonomous flying. In *Thesis* (Vol. 3727). https://infoscience.epfl.ch/record/95939/files/EPFL_TH3727.pdf

Bouabdallah, S., & Siegwart, R. (2005a). Backstepping and sliding-mode techniques applied to an indoor micro Quadrotor. *Proceedings - IEEE International Conference on Robotics and Automation*, *2005*, 2247–2252. https://doi.org/10.1109/ROBOT.2005.1570447

Bouabdallah, S., & Siegwart, R. (2005b). Towards Autonomous Indoor Micro VTOL. In *Autonomous Robots* (Vol. 18).

Bouabdallah, S., & Siegwart, R. (2007). Full control of a quadrotor. *IEEE International Conference on Intelligent Robots and Systems*, 153–158. https://doi.org/10.1109/IROS.2007.4399042

Bouzid, Y., Siguerdidjane, H., & Bestaoui, Y. (2017). Nonlinear internal model control applied to VTOL multi-rotors UAV. *Mechatronics*, *47*, 49–66. https://doi.org/10.1016/j.mechatronics.2017.08.002

Chamseddine, A., Zhang, Y., Camille, A. R., Canada, D., Join, E., Theilliol, D., Chamseddine, A., & Zhang, Y. M. (n.d.). *Flatness-Based Trajectory Planning/Replanning for a Quadrotor Unmanned Aerial Vehicle*.

Chen, F., Lei, W., Zhang, K., Tao, G., & Jiang, B. (2016). A novel nonlinear resilient control for a quadrotor UAV via backstepping control and nonlinear disturbance observer. *Nonlinear Dynamics*, *85*(2), 1281–1295. https://doi.org/10.1007/s11071-016-2760-y

Coza, C., & Macnab, C. J. B. (n.d.). *A New Robust Adaptive-Fuzzy Control Method Applied to Quadrotor Helicopter Stabilization*.

Dierks, T., & Jagannathan, S. (2010). Output feedback control of a quadrotor UAV using neural networks. *IEEE Transactions on Neural Networks*, *21*(1), 50–66. https://doi.org/10.1109/TNN.2009.2034145

Dong, W., Gu, G. Y., Zhu, X., & Ding, H. (2016). A high-performance flight control approach for quadrotors using a modified active disturbance rejection technique. *Robotics and Autonomous Systems*, *83*, 177–187. https://doi.org/10.1016/j.robot.2016.05.005

González-Sierra, J., Ríos, H., & Dzul, A. (2020). Quad-Rotor robust time-varying formation control: a Continuous Sliding-Mode Control approach. *International Journal of Control*, *93*(7), 1659–1676. https://doi.org/10.1080/00207179.2018.1526413

Hamza, A., Mohamed, A. H., & Ayman El-Badawy. (2022, January 3). Robust H-infinity Control for a Quadrotor UAV. *AIAA SCITECH 2022 Forum*. https://doi.org/10.2514/6.2022-2033

Hassanalian, M., & Abdelkefi, A. (2017). Classifications, applications, and design challenges of drones: A review. In *Progress in Aerospace Sciences* (Vol. 91, pp. 99–131). Elsevier Ltd. https://doi.org/10.1016/j.paerosci.2017.04.003

Hoffmann, G. M., Huang, H., Waslander, S. L., & Tomlin, C. J. (n.d.). *Quadrotor Helicopter Flight Dynamics and Control: Theory and Experiment* *.

Hoffmann, G. M., Huang, H., Waslander, S. L., & Tomlin, C. J. (2011). Precision flight control for a multi-vehicle quadrotor helicopter testbed. *Control*

Engineering Practice, *19*(9), 1023–1036. https://doi.org/10.1016/j.conengprac.2011.04.005

Hua, C., Chen, J., & Guan, X. (2018). Adaptive prescribed performance control of QUAVs with unknown time-varying payload and wind gust disturbance. *Journal of the Franklin Institute*, *355*(14), 6323–6338. https://doi.org/10.1016/j.jfranklin.2018.05.062

Jia, Z., Yu, J., Mei, Y., Chen, Y., Shen, Y., & Ai, X. (2017). Integral backstepping sliding mode control for quadrotor helicopter under external uncertain disturbances. *Aerospace Science and Technology*, *68*, 299–307. https://doi.org/10.1016/j.ast.2017.05.022

Katic, D., & Vukobratović, M. (2005). Survey of intelligent control algorithms for humanoid robots. *IFAC Proceedings Volumes (IFAC-PapersOnline)*, *16*, 31–42. https://doi.org/10.3182/20050703-6-cz-1902.01276

Kim, J., Gadsden, S. A., & Wilkerson, S. A. (2021). A Comprehensive Survey of Control Strategies for Autonomous Quadrotors. *Canadian Journal of Electrical and Computer Engineering*, *43*(1), 3–16. https://doi.org/10.1109/cjece.2019.2920938

Kim, J., Wilkerson, S. A., & Gadsden, S. A. (2016). Comparison of gradient methods for gain tuning of a PD controller applied on a quadrotor system. *Proceedings Volume 9837, Unmanned Systems Technology XVIII;*

Labbadi, M., Boukal, Y., & Cherkaoui, M. (2020). Path Following Control of Quadrotor UAV With Continuous Fractional-Order Super Twisting Sliding Mode. *Journal of Intelligent and Robotic Systems: Theory and Applications*, *100*(3–4), 1429–1451. https://doi.org/10.1007/s10846-020-01256-3

Labbadi, M., & Cherkaoui, M. (2019). Robust adaptive backstepping fast terminal sliding mode controller for uncertain quadrotor UAV. *Aerospace Science and Technology*, *93*. https://doi.org/10.1016/j.ast.2019.105306

Lee, D., Kim, H. J., & Sastry, S. (2009). Feedback linearization vs. adaptive sliding mode control for a quadrotor helicopter. *International Journal of Control, Automation and Systems*, *7*(3), 419–428. https://doi.org/10.1007/s12555-009-0311-8

Liu, H., Xi, J., & Zhong, Y. (2017). Robust Attitude Stabilization for Nonlinear Quadrotor Systems with Uncertainties and Delays. *IEEE Transactions on Industrial Electronics*, *64*(7), 5585–5594. https://doi.org/10.1109/TIE.2017.2674634

Liu, X., Gu, G., & Zhou, K. (1999). Robust stabilization of MIMO nonlinear systems by backstepping. *Automatica*, *35*(5), 987–992.

Ma, D., Xia, Y., Shen, G., Jia, Z., & Li, T. (2018). Flatness-based adaptive sliding mode tracking control for a quadrotor with disturbances. *Journal of the*

Franklin Institute, *355*(14), 6300–6322. https://doi.org/10.1016/j.jfranklin.2018.06.018

Moreno-Valenzuela, J., Perez-Alcocer, R., Guerrero-Medina, M., & Dzul, A. (2018). Nonlinear PID-Type Controller for Quadrotor Trajectory Tracking. *IEEE/ASME Transactions on Mechatronics*, *23*(5), 2436–2447. https://doi.org/10.1109/TMECH.2018.2855161

Mu, B., Zhang, K., & Shi, Y. (2017). Integral Sliding Mode Flight Controller Design for a Quadrotor and the Application in a Heterogeneous Multi-Agent System. *IEEE Transactions on Industrial Electronics*, *64*(12), 9389–9398. https://doi.org/10.1109/TIE.2017.2711575

Muñoz, F., González-Hernández, I., Salazar, S., Espinoza, E. S., & Lozano, R. (2017). Second order sliding mode controllers for altitude control of a quadrotor UAS: Real-time implementation in outdoor environments. *Neurocomputing*, *233*, 61–71. https://doi.org/10.1016/j.neucom.2016.08.111

Nettari, Y., Labbadi, M., & Kurt, S. (2023). Adaptive robust finite-time tracking control for quadrotor subject to disturbances. *Advances in Space Research*, *71*(9), 3803–3821. https://doi.org/10.1016/j.asr.2022.09.016

Nettari, Y (2023). *Robust control system design for non-linear systems* [Doctoral dissertation]. Yildiz Technical University Graduate School of Science And Engineering.

Noordin, A., Basri, M. A. M., & Mohamed, Z. (2019). Sliding mode control for altitude and attitude stabilization of quadrotor UAV with external disturbance. *Indonesian Journal of Electrical Engineering and Informatics*, *7*(2), 203–210. https://doi.org/10.11591/ijeei.v7i2.1149

Perruquetti, Wilfrid., & Barbot, J. Pierre. (2002). *Sliding mode control in engineering*. Marcel Dekker.

S. V. Emeryanov, S. K. Korovin, & A. Levant. (1996). High-Order Sliding Modes In Control Systems. *Computational Mathematics and Modeling*, *7*(3).

Shakhatreh, H., Sawalmeh, A. H., Al-Fuqaha, A., Dou, Z., Almaita, E., Khalil, I., Othman, N. S., Khreishah, A., & Guizani, M. (2019). Unmanned Aerial Vehicles (UAVs): A Survey on Civil Applications and Key Research Challenges. In *IEEE Access* (Vol. 7, pp. 48572–48634). Institute of Electrical and Electronics Engineers Inc. https://doi.org/10.1109/ACCESS.2019.2909530

Shao, X., Liu, J., & Wang, H. (2018). Robust back-stepping output feedback trajectory tracking for quadrotors via extended state observer and sigmoid tracking differentiator. *Mechanical Systems and Signal Processing*, *104*, 631–647. https://doi.org/10.1016/j.ymssp.2017.11.034

Shi, X., Cheng, Y., Yin, C., Dadras, S., & Huang, X. (2019). Design of Fractional-Order Backstepping Sliding Mode Control for Quadrotor UAV. *Asian Journal of Control*, *21*(1), 156–171. https://doi.org/10.1002/asjc.1946

Silvagni, M., Tonoli, A., Zenerino, E., & Chiaberge, M. (2017). Multipurpose UAV for search and rescue operations in mountain avalanche events. In *Geomatics, Natural Hazards and Risk* (Vol. 8, Issue 1, pp. 18–33). Taylor and Francis Ltd. https://doi.org/10.1080/19475705.2016.1238852

Slotine, J.-J. E. (Jean-J. E.), & Li, Weiping. (1991). *Applied nonlinear control*. Prentice hall Englewood Cliffs.

Tomic, T., Schmid, K., Lutz, P., Domel, A., Kassecker, M., Mair, E., Grixa, I., Ruess, F., Suppa, M., & Burschka, D. (2012). Toward a fully autonomous UAV: Research platform for indoor and outdoor urban search and rescue. *IEEE Robotics and Automation Magazine*, *19*(3), 46–56. https://doi.org/10.1109/MRA.2012.2206473

Utkin, V., Guldner, J., & Shi, J. (2017). *Sliding Mode Control in Electro-Mechanical Systems* (2nd ed.). CRC press.

Utkin, V. I. (1977). Variable Structure Systems with Sliding Modes. *IEEE Transactions on Automatic Control*, *22*(2), 212–222. https://doi.org/10.1109/TAC.1977.1101446

Utkin, V. I. (2013). *Sliding Modes in Control and Optimization*. Springer Science & Business Media.

Wang, H., Ye, X., Tian, Y., Zheng, G., & Christov, N. (2016). Model-free-based terminal SMC of quadrotor attitude and position. *IEEE Transactions on Aerospace and Electronic Systems*, *52*(5), 2519–2528. https://doi.org/10.1109/TAES.2016.150303

Wang, N., Deng, Q., Xie, G., & Pan, X. (2019). Hybrid finite-time trajectory tracking control of a quadrotor. *ISA Transactions*, *90*, 278–286. https://doi.org/10.1016/j.isatra.2018.12.042

Xue, W., Zhu, X., Yang, X., Ye, H., & Chen, X. (2021). A Moving Target Tracking Control of Quadrotor UAV Based on Passive Control and Super-Twisting Sliding Mode Control. *Mathematical Problems in Engineering*, *2021*. https://doi.org/10.1155/2021/6627495

Yang, H., Cheng, L., Xia, Y., & Yuan, Y. (2018). Active Disturbance Rejection Attitude Control for a Dual Closed-Loop Quadrotor under Gust Wind. *IEEE Transactions on Control Systems Technology*, *26*(4), 1400–1405. https://doi.org/10.1109/TCST.2017.2710951

Zadeh, L. A. (1965). Fuzzy S e t s *. In *INFOR~ATIO~ AND CONTROL* (Vol. 8).

Zhao, B., Xian, B., Zhang, Y., & Zhang, X. (2015). Nonlinear Robust Adaptive Tracking Control of a Quadrotor UAV Via Immersion and Invariance Methodology. *IEEE Transactions on Industrial Electronics*, *62*(5), 2891–2902. https://doi.org/10.1109/TIE.2014.2364982

Zou, Y., & Zhu, B. (2017). Adaptive trajectory tracking controller for quadrotor systems subject to parametric uncertainties. *Journal of the Franklin Institute*, *354*(15), 6724–6746. https://doi.org/10.1016/j.jfranklin.2017.08.027

Zuo, Z., & Ru, P. (2014). Augmented script L1 adaptive tracking control of quad-rotor unmanned aircrafts. *IEEE Transactions on Aerospace and Electronic Systems*, *50*(4), 3090–3101. https://doi.org/10.1109/TAES.2014.120705